https://doi.org/10.5194/egusphere-2026-6795
Preprint. Discussion started: 19 November 2026
© Author(s) 2026. CC BY 4.0 License.

Evaluating Sentinel-2 and PlanetScope Imagery for Detecting Ice Phenology in Alaskan Lakes and Ponds

Noah Jacobs[1], Sarah Cooley[1], Annie Cushman[1]

[1]Nicholas School of the Environment, Duke University, Durham, North Carolina, USA

Correspondence to: Noah Jacobs (nj142@duke.edu)

Abstract. Lake ice serves as both an indicator and driver of climate change, yet past studies have often overlooked ice phenology in small lakes and ponds due to the spatiotemporal limitations of existing satellite missions. Here we produce annual ice cover time series for 15,885 Alaskan lakes using high-resolution Sentinel-2 and PlanetScope imagery for the years 2019-2025. We assess the relative performance of both missions, then use our time series data to analyze the controls on lake ice timing across Alaska. We find that Sentinel-2 outperforms PlanetScope for ice phenology monitoring, especially at high latitudes, due to its superior revisit timing and improved classification performance. Planet's underperformance stemmed from its lower spectral resolution and overarching issues with its cloud mask. Our analysis of ice-on and ice-off timing demonstrates that large lakes maintain ice cover for, on average, 7 days longer than small ponds. This difference is primarily driven by delayed ice-off timing in large lakes, as ice-on took place synchronously across lake sizes. Climatologically, we confirm that the seasonal 0°C isotherm date is highly correlated with both ice-off and ice-on timing. We also find that lake ice cover responds more slowly to earlier warming in spring (and, conversely, faster to later cooling in fall), a moderate negative feedback which could dampen the number of lost ice cover days due to climate change. Overall, our findings reveal the value of high-resolution remote sensing data for studying lake ice dynamics in small lakes and emphasize Sentinel-2's particular utility for high-latitude observation.

1 Introduction

Seasonally ice-covered lakes and wetlands are some of the most dynamic and productive landscapes in the Arctic. They are key spaces for Northern communities who rely on ice cover for transportation, subsistence harvesting, and long-standing cultural practices (Hampton et al., 2024; Knoll et al., 2019). Lake ice serves as critical infrastructure in rural areas— frozen lakes are used to build ice roads for winter overland travel, and lakes are favored for snowmachine trails when traveling inland to hunt (Aporta, 2009; Hori et al., 2017; Mullan et al., 2021). Stable lake ice is also important for Arctic food sovereignty. Freshwater ice fishing has been a keystone winter subsistence food for centuries for many indigenous communities (Carothers et al., 2014; Moerlein & Carothers, 2012; Schott et al., 2020; Seigle et al., 2024). At a global scale, the timing of freshwater ice dynamics plays a major role in regulating the Arctic carbon cycle, as ice cover greatly reduces heat and gas exchange

https://doi.org/10.5194/egusphere-2026-6795
Preprint. Discussion started: 19 November 2026
© Author(s) 2026. CC BY 4.0 License.

between surface water and the atmosphere (Brown & Duguay, 2010). Northern lakes emit approximately 16.5 Tg of methane annually (comprising nearly 70% of all natural northern emissions), over a quarter of which takes place in the weeks immediately following ice-off (Jansen et al., 2019; Wik et al., 2016).

Across the Arctic, warming winter air temperatures are leading to the rapid decline of annual ice cover over lakes and wetlands. Globally, lakes have lost on average 28 days of ice cover over the last 150 years, and they are predicted to lose between 28 and 80 additional days of ice cover by the end of the century (Basu et al., 2024; Grant et al., 2021; Wang et al., 2022). This widespread loss of lake ice is pushing northern communities to adapt to shorter ice durations and declining fish populations (Cold et al., 2020; Knoll et al., 2019.; Woolway et al., 2022). Longer open water periods in the summer could also lead to increases in methane emissions (Guo et al., 2020; M. Kuhn et al., 2025; Wik et al., 2016), among many other key impacts (Hampton et al., 2024). Declining ice cover serves both as an indicator and an amplifier of climate change; when reflective ice gives way to open water, more shortwave radiation is absorbed, leading to net surface heating with cascading impacts on future ice formation (Cooley et al., 2026; X. Li et al., 2022). Since more than 86% of the Earth's 117 million lakes freeze on an annual basis (Korver et al., 2024), the positive feedback forcing from lake ice loss has significant implications for future warming. Understanding spatial and temporal patterns in ice cover changes across the Arctic is thus crucial for constraining climate impacts on northern ecosystems and communities.

Optical remote sensing can be a powerful tool for studying lake ice dynamics at a global scale, but past satellite missions have faced tradeoffs in spatial, temporal, and spectral resolution, limiting the scope of most lake ice studies. For instance, NASA's MODIS mission offers a high 1 to 2-day global revisit rate, which allows for rapid detection of ice cover changes, but its 250m spatial resolution results in the exclusion of all lakes smaller than 1 km² in large-scale lake ice studies (Šmejkalová et al., 2016; Wang et al., 2022; Wu et al., 2021; Zhang et al., 2021; Zhang & Pavelsky, 2019). Landsat sensors (ETM, OLI, TM) offer a potential compromise, with an extensive satellite record at 30 m resolution for long-term trend analysis. However, since this data is limited temporally to 16 or more days between observations, Landsat often has month-long or greater revisit windows in cloudy environments, which reduces the accuracy and utility of annual Landsat-derived ice phenology metrics (Barbieux et al., 2018; Nitze et al., 2017; Pickens et al., 2022; Wang et al., 2021; Yang et al., 2022).

While previous remote sensing studies have enabled new insights into lake ice phenology, existing sensor limitations have led to gaps in our understanding of the ice phenology of small lakes and of ice dynamics during the ice-on season. The literature's prevailing focus on large lakes overlooks a significant proportion of global surface water, as 94% of the world's lakes are smaller than 1 km², comprising approximately 15% of all lake area (Pi et al., 2022). This is important because small lakes and ponds play an outsized role in the global carbon cycle— they are estimated to emit methane at areal rates 5 to 10 times higher than large lakes, but they have been undercounted in global methane budgets (Holgerson & Raymond, 2016; M. Kuhn et al., 2025; Zhuang et al., 2026). Small lakes are also major drivers of seasonal surface water change (Mullen et al., 2023; Pi et al.,

https://doi.org/10.5194/egusphere-2026-6795
Preprint. Discussion started: 19 November 2026
© Author(s) 2026. CC BY 4.0 License.

2022) and are exceptionally important for global freshwater biodiversity (Biggs et al., 2017). The loss of ice cover in small lakes has cascading effects on wetland hydrology (Dolan et al., 2021), ecology (Smol & Douglas, 2007), and biogeochemistry (Martinsen et al., 2019). Furthermore, the ice-on season also has been largely understudied in the remote sensing literature, as low sun angles and thin ice conditions make it difficult to distinguish between ice and water in satellite imagery, reducing the utility of optical data (Heinilä et al., 2021; Wu et al., 2021). The prevailing focus on monitoring ice-off means that the contribution of ice-on timing to annual ice cover duration is understudied, particularly on a landscape scale. As autumn air temperatures rise rapidly across the globe, it will be important to constrain both ice-on and ice-off dynamics across a range of lake sizes to ensure we build an accurate understanding of how lake ice is changing in a warming world.

Advances in high resolution remote sensing technology over the past 10 years have vastly improved our abilities to study ice phenology of small lakes and ponds. Since 2017, the Sentinel-2 satellite constellation operated by the European Space Agency has offered a global sub-weekly revisit rate at as high as 10 m spatial resolution. Sentinel-2's temporal advantages are amplified in the Arctic, as orbital convergence towards the poles allows for near-daily revisit timing (J. Li & Roy, 2017). However, to date, studies using Sentinel-2 for high latitude lake ice monitoring have either focused solely on ice-off or excluded small lakes entirely in favor of large-scale trend analysis (Domart et al., 2024; Giroux-Bougard et al., 2023; Liu et al., 2021; Pletcher et al., 2025; Tong et al., 2024). Sentinel-2 thus offers new potential for monitoring the dynamics of ice in small lakes and ponds across the Arctic.

The recent development of commercial cube satellite constellations has also enabled new advancements in high resolution Arctic observation. Planet Labs operates a constellation of over 450 CubeSats, offering between 4 and 8 spectral bands at a ~3 meter spatial resolution, with a near-daily revisit rate worldwide. This high level of spatial and temporal detail has the potential to allow us to monitor rapid changes in the ice cover of small lakes (Cooley et al., 2017, 2019; Mullen et al., 2023). However, few studies have investigated the utility of PlanetScope for widespread monitoring of lake ice. The largest-scale study used PlanetScope data in conjunction with Sentinel-2 for monitoring ice-off and subsequent green-up across 35 lakes in Canada and Alaska (C. Kuhn et al., 2021). Other studies have been limited to low latitudes or only focused on the dynamics of a single lake (Gschwentner & Corman, 2023; Kouraev et al., 2021). No studies to date have used PlanetScope for monitoring lake ice-on (apart from Pickens et al. (2022), who used PlanetScope and Sentinel-2 sparingly as reference data to build Landsat-derived ice time series), nor have any studies assessed PlanetScope's applicability for large scale monitoring of ice-off dynamics. Planet offers higher spatial and temporal resolution than Sentinel-2, both characteristics that are particularly useful for monitoring ice phenology in small lakes. However, Sentinel-2 has better spectral and radiometric resolution, as well as vastly superior accessibility with all data made publicly available at no cost to the user. Understanding the comparative advantages and disadvantages of each sensor for lake ice phenology detection is thus valuable not only for the investigation of lake ice dynamics, but also more broadly for research on other Arctic and high-latitude processes requiring high spatial and temporal resolution.

https://doi.org/10.5194/egusphere-2026-6795
Preprint. Discussion started: 19 November 2026
© Author(s) 2026. CC BY 4.0 License.

In this study, we test the applicability of both PlanetScope and Sentinel-2 for monitoring lake ice-off and ice-on dynamics across three study sites in Alaska for the years 2019-2025. First, we identify ice phenology timing using red thresholding and random forest classification workflows. Next, we compare the accuracy and utility of both satellites by investigating revisit rates, cloud masking performance, and the accuracy of each satellite against hand labeled ice phenology dates. Finally, we examine the effects of morphology and climatology on ice dynamics, focusing on the influence of lake size, 0°C isotherm lag time, and air temperature on the timing and speed of ice cover changes. By examining both ice-on and ice-off dynamics in small lakes using high resolution remote sensing, we provide new perspectives on the relative utility of PlanetScope versus Sentinel-2 for high-latitude remote sensing, as well as new insight into the timing and controls of lake ice dynamics across Alaska.

2 Study Sites

We selected three 50×50 km study sites across Alaska, namely the Yukon-Kuskokwim Delta, Yukon Flats, and North Slope (Fig. 1), to enable examination of satellite performance and ice phenology across a range of latitudes, sun angle conditions, and local environmental/physiographic characteristics.

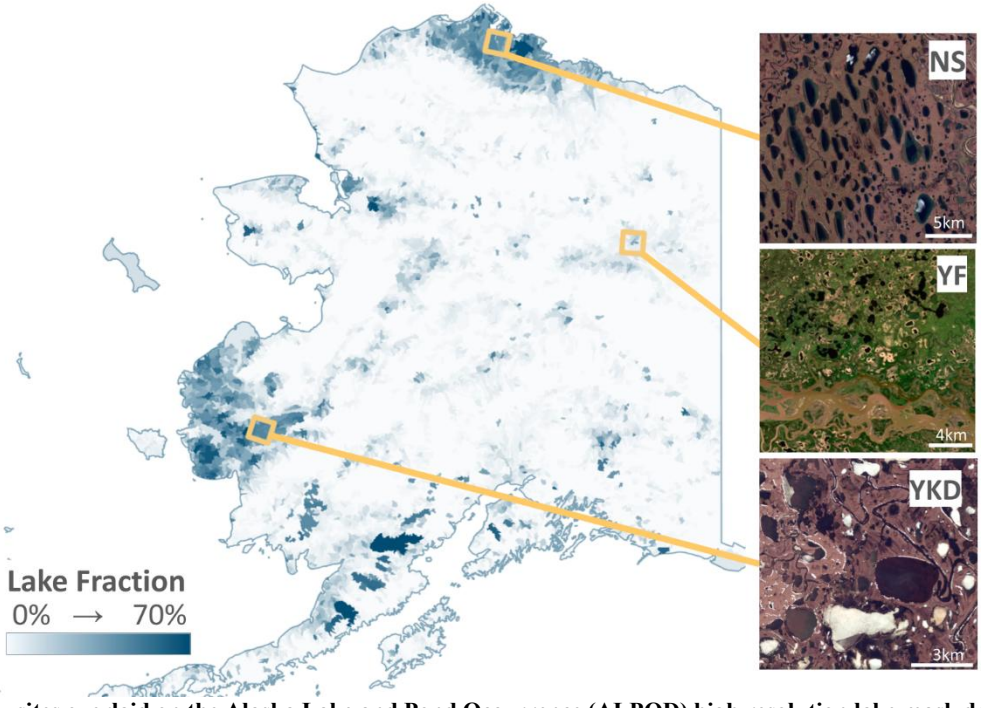


Figure 1: Study sites overlaid on the Alaska Lake and Pond Occurrence (ALPOD) high resolution lake mask dataset, shown in blue (Levenson et al. 2025). Lake polygons are aggregated to fraction of total watershed area for visibility at this scale. Watershed

https://doi.org/10.5194/egusphere-2026-6795
Preprint. Discussion started: 19 November 2026
© Author(s) 2026. CC BY 4.0 License.

boundaries sourced from the USGS Watershed Boundary Dataset, and Alaska outline sourced from the US Census Bureau TIGER/Line dataset. Note the attached PlanetScope images do not show the full 50x50 km study site extents; scale is reduced to highlight differences in landscape and lake morphology.

2.1 North Slope

The North Slope (NS) is a vast area of tundra stretching across the Alaskan coastal plain, containing hundreds of thousands of shallow (2-4m deep) thermokarst lakes. The region has been used by Iñupiaq hunters for subsistence hunting and fishing since time immemorial, and its frozen lakes remain an important component of safe winter overland travel and subsistence harvesting today. The lakes of the NS generally freeze to bedfast in winter, although rapid warming is shifting the region towards a regime dominated by thinner, floating ice (Arp et al., 2015; Surdu et al., 2015). The North Slope is the fastest warming region in Alaska due to polar amplification; it has already seen more than 0.5 ℃ of warming per decade since 1971 and will likely see 10°C of warming by the end of the century (Ballinger et al., 2023; Mizukami et al., 2022). The area has significant cloud cover year-round but is especially prone to cloudiness in the months between October and April (approximately 95% of winter days are mostly cloudy). The NS is also very cold year-round, with mean temperatures ranging from 4.4°C in July to -24.4°C in January. Temperatures generally stay below freezing between early October and late May.

2.2 Yukon Flats

The Yukon Flats (YF) is a dynamic system of lakes and wetlands surrounding the Yukon River in central Alaska. Its waterways have been continuously used by Gwich'in peoples for subsistence practices like hunting, fishing, and gathering for over six millennia (Kofinas et al., 2010). Many of the region's lakes and ponds are highly interconnected through subsurface channels of thawed permafrost, as well by intermittent processes like spring ice jam flooding (Rey et al., 2019). The YF has moderate year-round cloud cover, with little seasonal variation; more than 60% of days have at least partial cloud cover. The area has an extreme seasonal temperature range from 16.7°C in July to -26.7°C in January, with temperatures generally staying below 0° between late September and late April. Notably, the YF is prone to major seasonal temperature variation and has held records for both the highest and lowest temperature in Alaska (Wendler et al., 2017).

2.3 Yukon-Kuskokwim Delta

The Yukon-Kuskokwim Delta (YKD) is an approximately 72,800 km² area of wetlands in southwest Alaska, home to the largest intertidal wetland in North America and one of the largest populations of indigenous peoples in the Arctic. The landscape has been widely used for hunting, trapping, and fishing for thousands of years by Yup'ik subsistence hunters, who continue to adapt to the effects of sea level rise, flooding from severe storms, and ongoing ecological shifts (Jorgenson et al., 2025). The region hosts a variety of lake morphologies impacted by thermokarsting, river connectivity, and ongoing drainage events driven by thawing permafrost (Jorgenson et al., 2025). Over 99% of the region's 148,000 lakes are smaller

https://doi.org/10.5194/egusphere-2026-6795
Preprint. Discussion started: 19 November 2026
© Author(s) 2026. CC BY 4.0 License.

than 1 km², but these small lakes compose only around 46% of surface water area in the region (Pletcher et al., 2025). It is cloudy year-round in the YKD (around 80% of days see at least partial cloudiness), and there is little significant seasonal variability in cloud cover. The average temperature ranges from 17.8°C in July to -13.3°C in January, with temperatures generally staying below 0°C between October and late April.

3 Methods

3.1 Data

Central to accurate detection of lake ice phenology in small lakes is a high-resolution static water mask. To identify lake areas, we used the 10m resolution Alaska Lake and Pond Occurrence (ALPOD) dataset (Levenson et al. 2024; Levenson et al., 2025). This dataset was created from Sentinel-2 imagery using a U-Net model to classify open water occurrence in all lakes and ponds across Alaska as small as 0.001 km². For the purposes of this study, we used the ALPOD vector product, in which more than 800,000 individual lake polygons were created by applying a 25% seasonal water occurrence threshold to the corresponding raster dataset. ALPOD offers a much higher spatial resolution than available global-scale water masks and therefore enables us to investigate small lakes that are not present in Landsat-derived surface water products. We clipped ALPOD to each of our 50x50 km study regions, resulting in lake polygons for 5,694 lakes in the North Slope (NS), 1,858 in the Yukon Flats (YF), and 8,333 in the Yukon-Kuskokwim Delta (YKD).

We compared the benefits and drawbacks of PlanetScope and Sentinel-2 data for lake ice monitoring to understand the relative advantages and disadvantages of each satellite's temporal, spatial and spectral resolution. For Planet, we downloaded both 4-band and 8-band Surface Reflectance scenes with corresponding UDM-2 data quality masks. For Sentinel-2, we limited our analysis to Level-2A scenes sourced from the Element 84 Earth Search Catalogue to ensure all data was atmospherically corrected and contained a Scene Classification Layer raster (SCL). We downloaded all available ice-off and ice-on imagery within a 50x50 km bounding box for each study site between the years 2019-2025. We approximated the start and end dates of each shoulder season using a quick visual inspection on Planet Explorer, giving at least one month of leeway on either side to account for potential interannual variation of ice-on and ice-off dates.

3.2 Cloud Cover Filtering

Due to necessary differences in ice-on vs. ice-off processing approaches (see below), we used two separate workflows to filter clouds from our Sentinel-2 dataset. For Sentinel-2, previous remote sensing studies have successfully used generous cloud cover thresholds for identifying ice (Liu et al., 2021), so we selected an 85% full scene cloud cover threshold in both seasons and relied on cloud probability masks to filter out unusable pixels within each image. For ice-off, we used both the Scene Classification Layer (SCL) and s2cloudless rasters hosted on Google Earth Engine to filter out cloudy pixels from our dataset. For ice-on, since random forest classification was performed on a local compute cluster with atmospherically corrected L2A

https://doi.org/10.5194/egusphere-2026-6795
Preprint. Discussion started: 19 November 2026
© Author(s) 2026. CC BY 4.0 License.

data, we instead used SCL with OmniCloudMask (Wright et al., 2025), as running s2cloudless locally would have required substantial additional raw L1C data for each scene, which would have significantly increased compute cost.

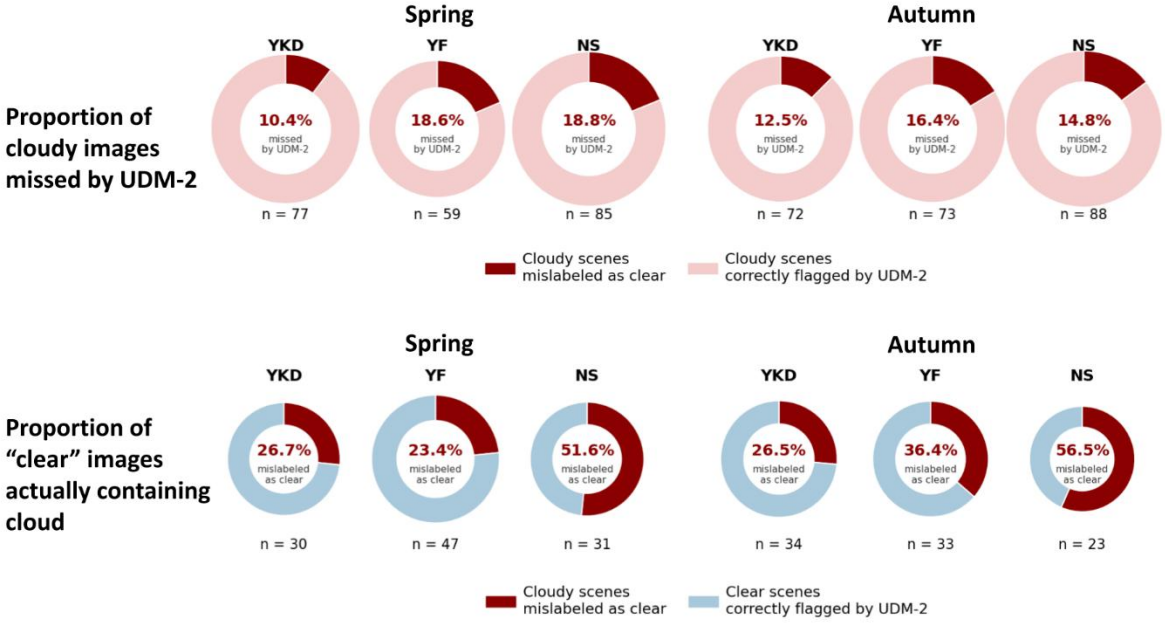


Figure 2: Planet UDM-2 cloud mask failure rates calculated from 100 randomly selected images per site/season. Top row shows the proportion of cloudy images missed by UDM-2, demonstrating a consistent ~15% failure rate across Planet's UDM-2 cloud mask regardless of season or snow cover. Although not shown in this figure, we found the same patterns held in summer, indicating that rates of cloud mask failure were not limited to failure in snowy conditions. Bottom row shows proportion of downloaded clear imagery which actually contained cloud, indicating that UDM-2's failure rates lead to as high as 51.6% unusable data in cloudier sites (NS, n=31).

To filter clouds from PlanetScope imagery, we first began by manually investigating the accuracy of Planet's UDM-2 cloud mask, as it has been found to be unreliable in high-latitude environments (Z. Li et al., 2026). We selected a validation sample of 900 randomly selected images, distributed evenly across three seasons (ice-off, ice-on, and summer) and stratified across each of our three study sites. We used an initial 85% cloud cover threshold to test both the proportion of cloudy images missed by UDM-2 and the proportion of clear images (according to UDM-2) which were contaminated by cloud cover.

In sites with fewer clear days (e.g. the North Slope), we found that errant cloudy scenes were so prevalent, they outnumbered true clear scenes (Fig. 2). Even when limiting Planet image selection to only images with metadata labels of 0% cloud cover, we found that cloud error still accounted for approximately 20% of our image quota. Thus, we limited our Planet downloads

https://doi.org/10.5194/egusphere-2026-6795
Preprint. Discussion started: 19 November 2026
© Author(s) 2026. CC BY 4.0 License.

to a strict 0% cloud cover filter, and then manually validated all 17,368 "cloud-free" PlanetScope scenes by hand. We confirmed the errant presence of clouds in over 23% of these scenes, and removed all images where missed cloud pixels would disrupt a significant proportion of observed lakes.

3.3 Spring Ice-off Classification

Previous studies of spring ice-off have used a variety of classification schemes for ice detection. One common method is red thresholding, in which ice is classified using reflectance values in the red band to distinguish bright ice from dark water (Cooley & Pavelsky, 2016; Pletcher et al., 2025; Zhang et al., 2021; Zhang & Pavelsky, 2019). Another common strategy is machine learning, in which more complex models are trained to recognize spectral signatures of various surfaces, which allows users to distinguish ice from water or sediment (Domart et al., 2024; Giroux-Bougard et al., 2023; Nguyen et al., 2026; Yang et al., 2022). We investigated the accuracy of both random forest and red thresholding models for pixel-wise classification using a validation dataset of twenty-three hand-classified ice-off scenes. We found both methods exhibited similar accuracy, with random forest achieving 97.0% and red thresholding achieving 96.3% per-pixel accuracy over our training dataset of over 156 million pixels. As red thresholding was substantially faster and more computationally efficient with similar accuracy, we selected red thresholding for our ice-off workflow.

To find the optimal red band reflectance threshold to distinguish ice from water, we performed a binary search optimization using a hand-classified validation dataset, and found both satellites had an optimal reflectance threshold of 0.095. This is consistent with previous studies using Sentinel-2 for ice monitoring (Pletcher et al., 2025). After filtering both image datasets for cloud cover, we clipped each scene to the ALPOD vector product, and calculated ice percentage for each observed lake. Applying this classification across our satellite record allowed us to build time series of ice cover across all lakes within our study sites. Our red-thresholding-derived time series dataset had a total of 6.5 million total lake ice-off observations between 2019-2025 across the YKD, YF, and NS.

3.4 Autumn Ice-on Classification

https://doi.org/10.5194/egusphere-2026-6795
Preprint. Discussion started: 19 November 2026
© Author(s) 2026. CC BY 4.0 License.

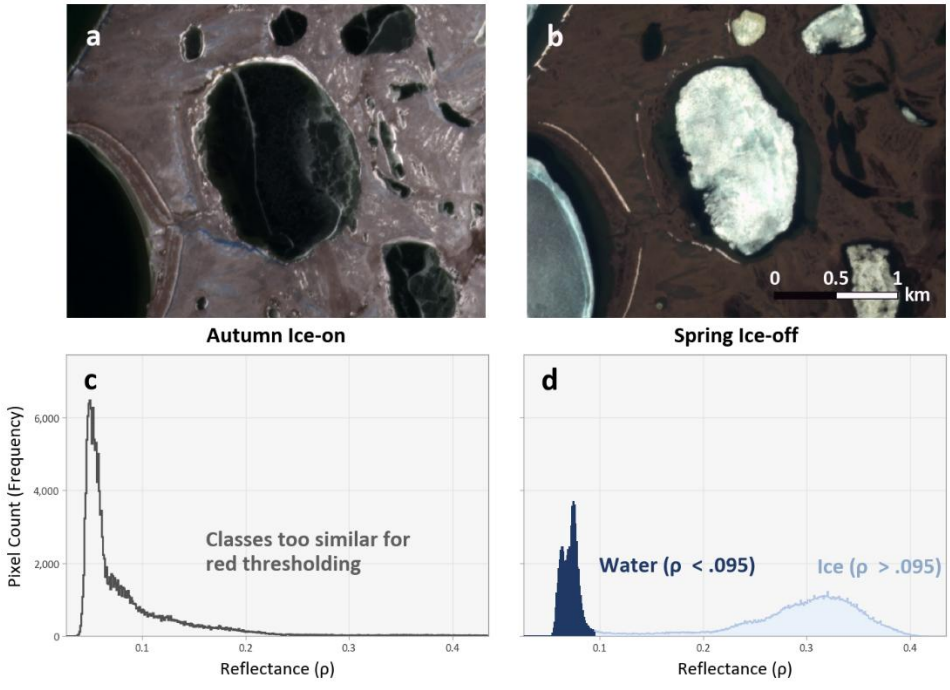


Figure 3: Comparison of ice-off and ice-on image histograms from the North Slope showing why low sun angles and optically thin ice prevents the use of traditional red thresholding methods during the ice-on season. A PlanetScope image during ice-off (b), captured 10/04/2023 at 70° 22' 51"N 155° 09' 09"W, shows thick, snowy ice cover, with a clear spectral divide between ice and water which allows red thresholding across the image histogram (d). Alternatively, image (a), captured 06/27/2025, shows how ice-on occurs during lower sun angle conditions with thinner, darker ice, leading to a lack of clear separation between histogram classes (c). Note both histograms were limited only to pixels within lake boundaries.

Ice classification during the ice-on season is substantially more difficult than ice-off for two reasons. First, ice in the fall begins as a single thin, dark layer, and has close spectral similarity to water. Second, low sun angles in autumn reduce the overall contrast in image histograms, further preventing clear separability during ice-on (Fig. 3). Given this, red thresholding was not feasible for ice-on, so we instead trained site-specific random forest models for ice detection.

Past studies have successfully used machine learning for classifying ice-on ice cover in large lakes >1 km² (Domart et al., 2024; Tong et al., 2024). We trained random forest models for both Sentinel-2 and PlanetScope, using hyperparameter tuning with GridSearchCV to identify optimal configurations specific to each satellite. For Planet, the best model had 400 trees with no max depth, and a minimum split size of five. This configuration achieved a moderate overall test accuracy of 90.3% with 95,796 training samples. Findings indicated that the Planet model was slightly biased towards predicting water, as it tended to underrecognize darker ice surfaces, resulting in a lower recall for the ice class; it misclassified approximately 13% of ice pixels as water. We attribute this to Planet's more limited spectral range. For Sentinel-2, the tuned model used 500 trees with no max

https://doi.org/10.5194/egusphere-2026-6795
Preprint. Discussion started: 19 November 2026
© Author(s) 2026. CC BY 4.0 License.

depth, and a minimum split size of two, producing higher overall performance. We ran these models on our final ice-on time series dataset, for a total of 9.3 million total lake ice-on observations between 2019-2025.

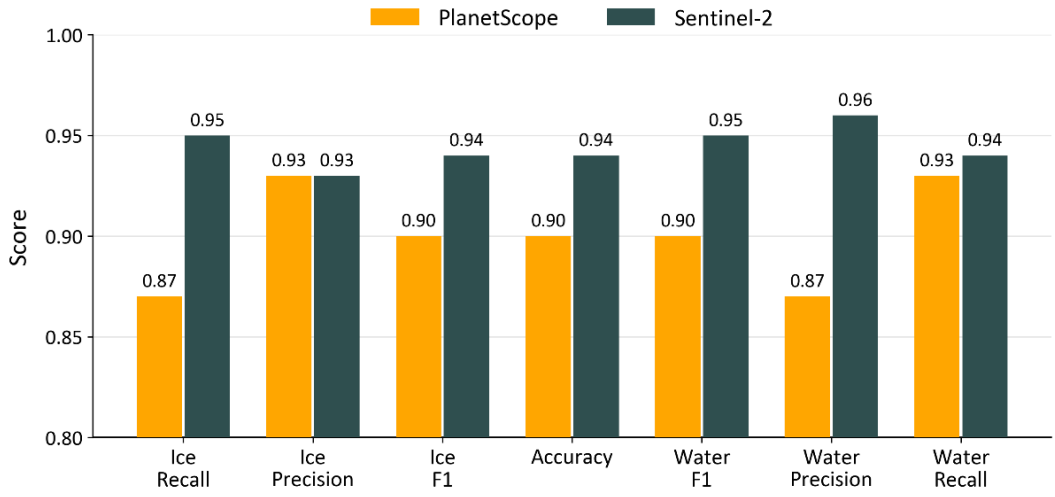


Figure 4: Random Forest performance metrics for PlanetScope (orange) and Sentinel-2 (blue), evaluated against our manually labeled validation dataset. Sentinel-2's random forest model outperformed or matched Planet across all metrics, with 94% overall accuracy for Sentinel and 90% overall accuracy for Planet.

3.5 Ice-on and Ice-off Date Detection

To detect ice-on and ice-off dates, we began by processing time series of ice and water fraction, which we refined using a series of logical filters to reduce the influence of misclassified pixels. First, we removed any lake observations partially obscured by cloud, as we found even with successful cloud masking, hazy edge pixels often still leaked into our filtered time series. Second, for ice-on, we filtered out drained lake beds by removing any time series with no ice pixels detected across the entire shoulder season. Third, we aggregated all time series to a single observation per day by selecting the image with the lowest ice cover. We chose lowest ice cover as our aggregation metric because errant cloud shadows over ice were rarely classified as water, while errant cloud pixels over water were frequently classified as ice; this helped to remove any last patches of haze missed by our cloud masking workflow. Finally, we removed any remaining single-day spikes in ice cover (e.g. any point where percent ice cover jumped more than 75% in a single day and then immediately returned to baseline) as a final backstop to prevent any one-off cloudy observations from disrupting our time series.

To determine the approximate date of ice-off for each lake-year, we interpolated between cloud-free observations within our time series to find the first occurrence when each lake passed a 75% open water threshold. Previous studies have used various thresholds for determining ice-off dates, but these thresholds usually fall between 75% to 90% open water coverage (Pavelsky & Smith, 2004; Pletcher et al., 2025; Zhang et al., 2021; Zhang & Pavelsky, 2019). We used the same 75% water cover threshold as Pletcher et al (2025), who found it was sufficient to mitigate edge effects in small lakes caused by mixed pixels.

https://doi.org/10.5194/egusphere-2026-6795
Preprint. Discussion started: 19 November 2026
© Author(s) 2026. CC BY 4.0 License.

We applied the inverse logic for ice-on detection, selecting the latest occurrence of 75% ice coverage as the ice-on date for each lake-year. In our lower latitude sites, lakes often fluctuated above and below this 75% threshold during the ice-on process, so we selected the latest occurrence of ice-on to ensure all ice duration estimations were continuous. We calculated uncertainty for each metric by averaging the distance to a usable observation on either side of the estimated ice phenology date. If a lake had more than ±15 days of uncertainty for a given year, we removed that observation and counted that season as undetected for the lake-year in question.

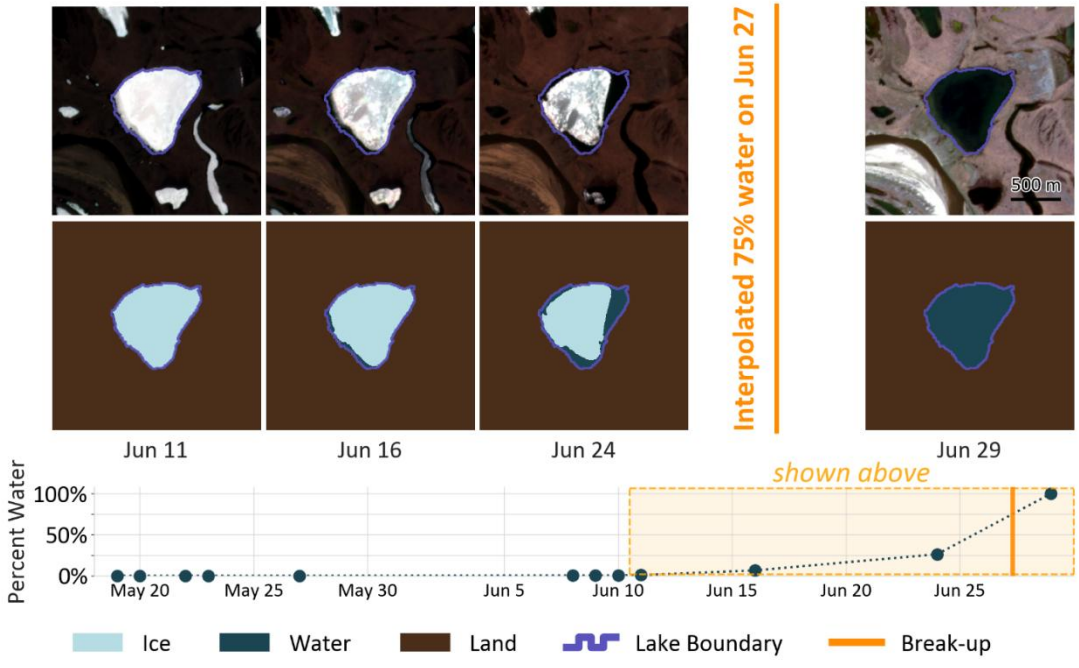


Figure 5: Example ice ice-off time series interpolation for ALPOD lake 495945 (70.499°N, 155.049°W) in the North Slope, 2023. RGB PlanetScope scenes are shown along the top row, with the ALPOD-derived lake boundary highlighted in blue, and pixel-wise red threshold classifications shown below each image distinguishing ice (light blue) from water (dark cyan). Aggregated % water cover for each observation is shown below the image on the y-axis as points along the time series.

To verify our detected ice-on and ice-off dates, we hand labeled a sample of 1,500 time series of ice cover across both seasons, combining data from both satellites to manually estimate the true ice-off and ice-on dates for each site. These hand-labeled ice-off and ice-on dates were used in place of a ground truth dataset, allowing us to estimate the temporal accuracy of both satellites in ice cover change detection.

3.6 Drivers of Ice Phenology

To understand the geophysical factors driving ice phenology, we investigated the relationship between lake morphological variables and ice timing, focusing on both shoreline complexity and lake area. We used the bias-corrected shoreline development index (Seekell et al., 2022) to analyze the relationship between shoreline complexity and ice phenology timing,

https://doi.org/10.5194/egusphere-2026-6795
Preprint. Discussion started: 19 November 2026
© Author(s) 2026. CC BY 4.0 License.

as shoreline complexity has been found to play a significant role in the dynamics of lake ice due to increased thermal contact with land area and differences in wind fetch (Sharma et al., 2019). We chose the bias-corrected index because normal shoreline development indices do not account for variation in lake size and the fractal nature of shorelines, which leads to bias with growing lake size.

Next, to analyze the effects of lake surface area on ice timing, we used lake sizes calculated from ALPOD, binned by small (<0.01 km²), medium (0.01-0.5 km²) and large (>0.5 km²) lakes. We chose a distribution skewed towards smaller lakes to investigate the spatial resolution limits of high-resolution remote sensing for lake ice monitoring; our dataset was uniquely positioned to investigate whether Planet offers meaningful differences with its ~3m pixel size vs. Sentinel-2's ~10m resolution. Furthermore, we assessed the role of lake size using Cuzick's test across continuous lake size distributions, which reinforced the results of our binned calculations.

We also investigated the relationship between air temperature amd ice phenology timing. In previous studies, near-surface air temperature has been found to be the most important driver of ice phenology changes, but varying metrics have been used to quantify those effects (Pletcher et al., 2025; Sharma et al., 2019; Šmejkalová et al., 2016). We therefore investigated three common metrics using ERA-5 T2m reanalysis data: accumulated degree days, mean 30d temperature, and 0°C isotherm DOY. We calculated accumulated degree days by selecting the earliest ice-on and ice-off dates for each site, which we used to estimate the endpoint of a fixed 30-day window to quantify the number of degree days past the 0°C threshold accumulated each year. We also used this same 30-day window to aggregate mean temperatures for each of our study sites. Finally, we calculated the 0°C isotherms for each year by taking the first 5-day window where ERA-5 mean T2m temperatures were at or above 0°C (for spring) or at or below 0°C (for fall). We tested the wider 31-day moving isotherm window used by previous studies (Bonsal & Prowse, 2003; Šmejkalová et al., 2016) and found the smaller 5-day window exhibited stronger correlation for our data. We then used these isotherm dates to calculate the number of "lag days" between the isotherm dates and ice-on/ice-off dates, following the methodology of Pletcher et. al (2025). Notably, we assessed isotherm lag timing not just for ice-off but also for ice-on, as lag timing after the fall isotherm has not been widely examined due to the scarcity of ice-on studies.

4 Results

4.1 Ice-on and Ice-off Timing

We estimated ice-on and ice-off dates across 15,885 Alaskan lakes for the years 2019-2025. For ice-on, moving northward led to progressively earlier mean ice-on dates (YKD Oct 29th ±6.1 days, YF Oct 15th ±5.0 days, NS Oct 8th ±4.4 days ; mean ± standard deviation, results averaged from both Planet and Sentinel-2) keeping with the expectation that higher latitude sites are colder with reduced incoming solar radiation, and therefore freeze before low latitude sites. However, despite large differences in latitude, both the YKD and YF have similar mean ice-off timing (May 16th ±9.8 days in the YKD vs May 14th

https://doi.org/10.5194/egusphere-2026-6795
Preprint. Discussion started: 19 November 2026
© Author(s) 2026. CC BY 4.0 License.

±7.7 days in the YF) while ice-off in the NS occurred almost a month later (on average June 16th. ±7.2 days) This pattern follows the difference in continental versus oceanic climate; the YF is much colder in the fall and winter than the YKD, but they have similar air temperatures in spring despite the YF being hundreds of kilometers further north. Overall, we find that mean annual ice duration increases with latitude; mean ice-cover days are approximately 251 ±8.1 days in the NS, 212 ±9.4 days in the YF, and 198 ±10.7 days in the YKD. These results show strong agreement with previous estimates of ice duration across the NS (Nguyen et al. 2026).

The NS had the largest interannual variation in ice-on timing across our 7-year record, with the earliest mean DOY detected on September 13th in 2021, and on October 7th in 2025. The YF had the least variation, with mean ice-on across all years occurring between October 10th and 21st. The YKD, meanwhile, had the largest interannual variation in ice-off timing, ranging between May 4th in 2019 and May 28th in 2023. The NS saw the smallest variation, with all years on record taking place between June 11th and 21st.

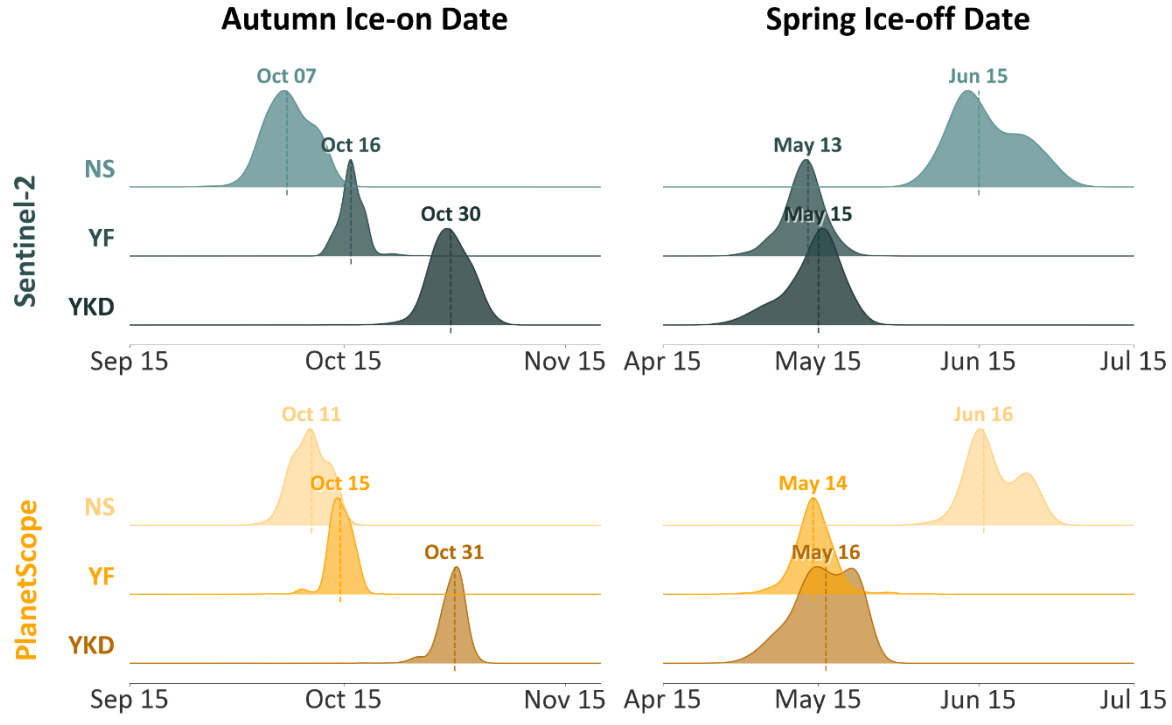


Figure 6: Kernel density plots of ice-off and ice-on derived from Sentinel-2 (top row, blue) and PlanetScope (bottom row, orange) using the median phenology dates for each lake across all years in our dataset. In total, Sentinel-2 observed ice-off for 110,072 lake-years and ice-on for 74,909 lake-years across the three study sites, whereas Planet observed ice on in 100,954 and ice-on in 70,794 lake-years. The y axis shows cumulative median observations over 2019-2025 for each Alaskan study site; the North Slope (NS),

https://doi.org/10.5194/egusphere-2026-6795
Preprint. Discussion started: 19 November 2026
© Author(s) 2026. CC BY 4.0 License.

Yukon Flats (YF), and Yukon-Kuskokwim Delta (YKD). Distributions between the two sensors show general agreement within ±3 days.

Our results indicate that ice-on took place more synchronously than ice-off within each of our study sites. IQRs for ice-on across both satellites were between 6-10 days for each of our regions, while IQRs for ice-on fell below the functional temporal resolution across all three sites (around 2 days for YKD and YF). In other words, all lakes within each study region tended to freeze simultaneously, whereas ice-off occurred over a longer window. This difference suggests that ice-on within a given region is controlled by a regional-scale forcing, with lakes tending to freeze together all at once, while ice-off is controlled by lake-specific morphological variables over a longer shoulder period.

4.2 Observational Success & Effective Revisit Intervals

Averaged across all study sites, we find that Sentinel-2 had superior observational success rates for ice phenology monitoring. Sentinel-2 successfully observed 96% of potential ice-off events with a mean uncertainty of ±3.3 days, and 67% of ice-on events with a mean uncertainty of ±5.4 days (Fig. 7). Planet, alternatively, observed 87% of potential ice-off events with a mean uncertainty of ±3.5 days, and 60% of ice-on events with a mean uncertainty of ±5.3 days. We found reduced observation rates during autumn ice-on across both satellites. The North Slope had the lowest overall success rates, with both satellites failing to detect almost two thirds of potential ice-on dates, primarily due to high cloud cover particularly in 2020 and 2021. Notably, Sentinel-2 was able to observe over 90% of potential ice-on events in the Yukon Flats, while Planet was only able to detect 67%, as Planet had two years (2022 and 2025) with essentially no ice-on observations. This is likely an artifact of Planet's small swath width and poor cloud masking leading to much more sporadic revisit timing, especially in cloudy environments.

At our highest latitude sites, the North Slope and Yukon Flats, we find that Sentinel-2 reliably outperformed Planet in mean effective revisit interval (ERI), which we define as the average number of days between usable, cloud-free observations within a season (Fig. 7). Sentinel-2 performed best during ice-off; Sentinel-2's mean ice-off ERI across all sites was 6.4 days, while Planet's was 8.3 days. Meanwhile, for ice-on, both satellites' observational frequency was significantly worsened by cloud cover, especially in the North Slope, but PlanetScope (26.3 day ERI) still significantly underperformed Sentinel-2 (12.2 day ERI). Nonetheless, Planet exhibited improved performance in our lowest latitude study site, the Yukon-Kuskokwim Delta (61.2°N). During the ice-off season in the YKD, Planet's performance was improved with 6.8 days ERI vs. Sentinel-2's 8.8 days, and the constellation also approximately matched Sentinel-2 during the YKD's ice-on season (Planet 12.2 days ERI vs. Sentinel-2 12.4 days). Our results indicate that at very high latitudes and in cloudy environments, Sentinel-2 offers more regular and reliable observational frequency, but Planet's temporal advantages increase moving southward.

https://doi.org/10.5194/egusphere-2026-6795
Preprint. Discussion started: 19 November 2026
© Author(s) 2026. CC BY 4.0 License.

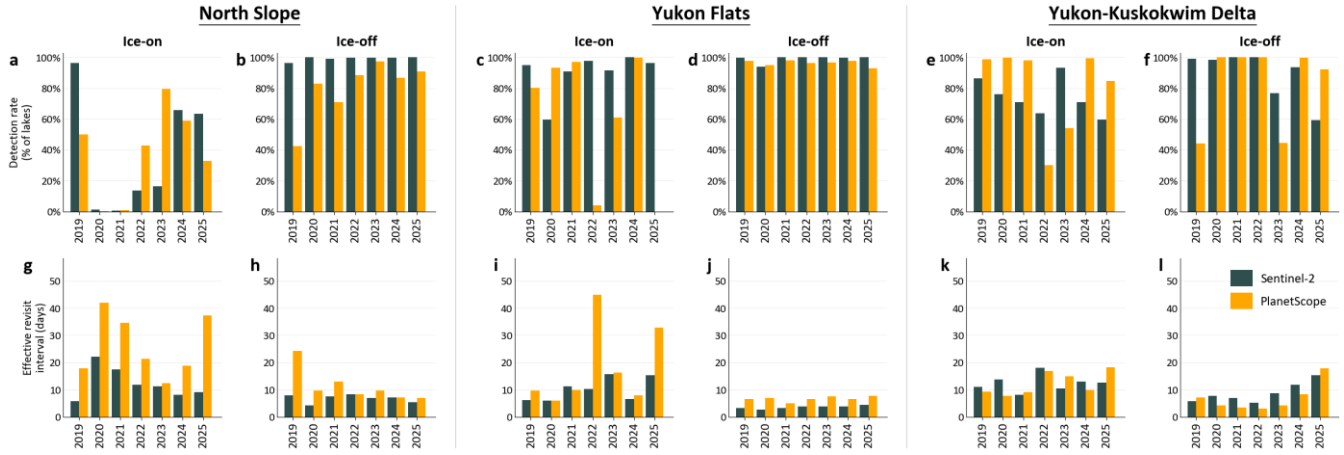


Figure 7. Bar charts comparing the ice phenology detection rates and effective revisit intervals (ERIs) for both PlanetScope and Sentinel-2. ERI values for each site were calculated by taking the mean number of days between valid observations (e.g. those which survived our quality filtering) in each lake, then averaging those values annually across each 50x50km study site. A shorter ERI indicates that a satellite captured usable imagery more frequently over the course of the season, while a higher detection rate indicates that a greater percentage of lakes successfully had ice-on or ice-off observed within a given year. Both metrics inherently include the effects of cloudiness, as only successful observations are included in our calculations. Note that both ice-on and ice-off detection rates are shown as percent of lakes observed to preserve inter-site comparability; total lake numbers are 5,694 for the North Slope, 1,858 for the Yukon Flats, and 8,333 for the Yukon-Kuskokwim Delta.

4.3 Manual Accuracy Assessment

https://doi.org/10.5194/egusphere-2026-6795
Preprint. Discussion started: 19 November 2026
© Author(s) 2026. CC BY 4.0 License.

When compared against manually validated ice-off and ice-on dates, we find that Sentinel-2 exhibited superior accuracy to Planet across nearly all sites and seasons. Out of 1,500 sampled time series, Sentinel-2's interpolated ice phenology dates were on average 1.2 days closer to our hand-labeled dates, with the sole exclusion of the YKD during ice-on, where Sentinel had a MAE of 5.4 days against Planet's 4.4 days, and a RMSE of 8.4 days vs Planet's RMSE of 6.4 days. Planet's improved performance in the YKD is likely an artifact of orbital divergence at lower latitudes reducing Sentinel-2's comparative revisit rate, on top of the less-cloudy conditions in the YKD allowing for a greater proportion of usable Planet imagery.

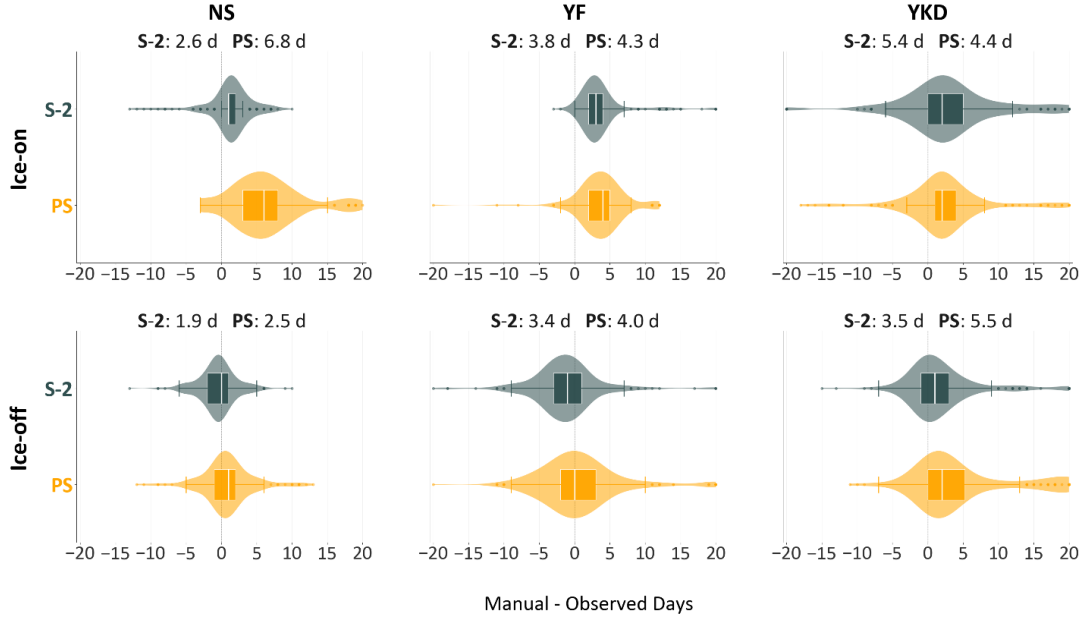


Figure 8. Box and violin plots representing the deviation from manually validated ice phenology dates for both Planet (PS) and Sentinel-2 (S-2). Subheadings show Mean Absolute Error (MAE) for each sample. n=250 for each study-site and season.

4.4 Morphological Drivers of Ice Phenology

We find larger lakes see ice-off on average 6 to 10 days later than small lakes across all study sites, but we do not observe a consistent pattern with lake size for ice-on. Cuzick's test showed significant positive correlation between ice-off timing and lake area for both Planet and Sentinel-2. For ice-on, we find that larger lakes in the NS took on average 8 days longer than small lakes to freeze, following a similar size distribution trend to ice-off. However, in the YF and YKD, we did not identify statistically significant relationships between lake size and ice-on timing. We hypothesize this disparity is due to the influence of complex climatological and morphological factors, including dark ice formation, anisotropic ice patterns caused by wind in large lakes, and multiple freeze-thaw dates within a single season.

Similarly, we find that large lakes had on average 7.1 days longer mean annual ice duration than small lakes across our three study regions. Interestingly, the difference in ice duration between large and small lakes did not vary significantly between

https://doi.org/10.5194/egusphere-2026-6795
Preprint. Discussion started: 19 November 2026
© Author(s) 2026. CC BY 4.0 License.

sites; large lakes had ice durations of 8.3 (NS), 6.1 (YF) and 6.9 (YKD) longer than small lakes across all years. Linear regression of duration vs. size across our full dataset indicates that for each additional km² of lake area, annual ice cover lasts 2.4 days longer, which we primarily attribute to larger lakes being slower to respond to thermal forcing in spring.

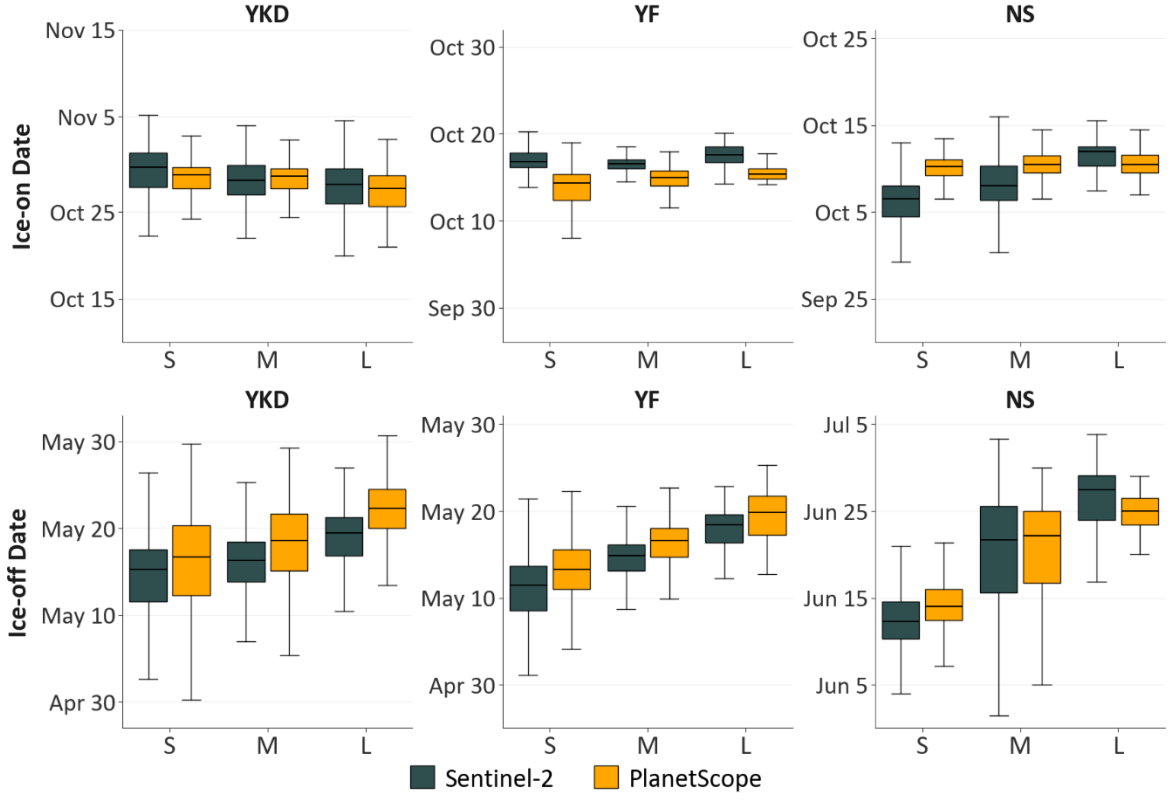


Figure 9: Box plots of ice-on and ice-off dates binned by lake size, indicating trends between small (< 0.01 km², medium (0.01 – 0.5 km²), and large (> 0.5 km²) lakes. Note that there are significantly fewer large lakes, (n = 44 to 245), than medium lakes (n = 894 to 3489) and small lakes (903 to 4642). Only lakes observed by both satellites are included in this figure to ensure comparability. Outlier points excluded from this figure to keep axes legible.

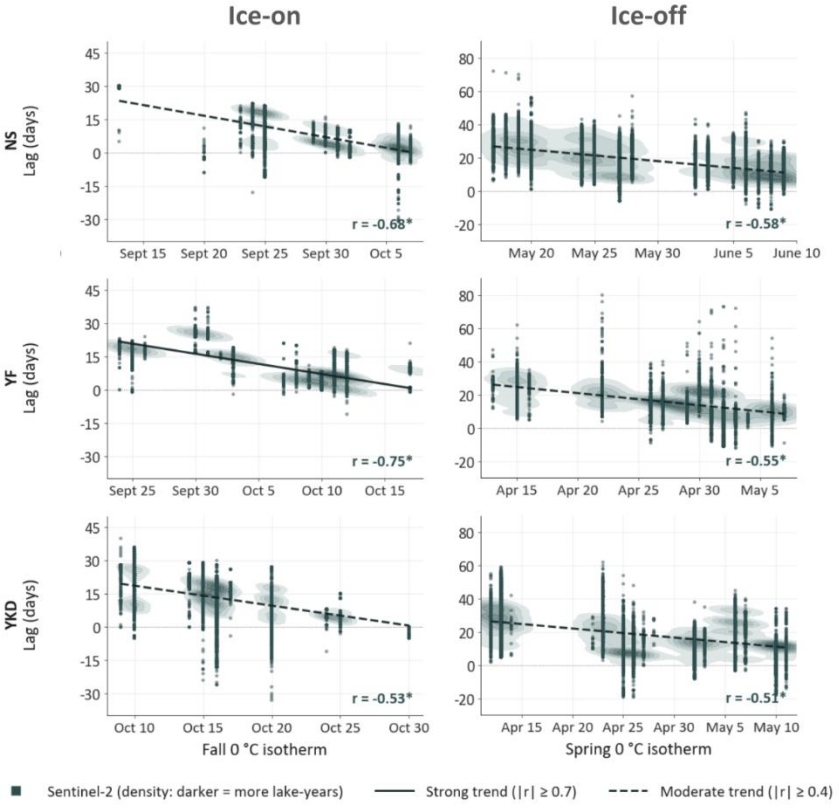
Our results show that shoreline complexity did not have a major impact on ice phenology timing across our three study sites. For ice-off, although rougher-shored lakes exhibited a weak pattern of melting out slightly earlier (ρ = -0.10 to -0.17), bias-corrected shoreline development index (SDI_{bc}) explained less than 2% of overall variance. For ice-on, no consistent pattern emerged, and the direction of correlation changed between sites. This indicates that shoreline complexity had no generalizable effect on seasonal ice timing within our study regions.

https://doi.org/10.5194/egusphere-2026-6795
Preprint. Discussion started: 19 November 2026
© Author(s) 2026. CC BY 4.0 License.

4.5 Climatic Drivers of Ice Phenology

Out of the three temperature metrics tested (0°C isotherm, accumulated degree days, and mean 30d air temperature), we found that the spring and autumn 0°C isotherm dates exhibited the strongest correlation with ice phenology timing. The 0°C isotherm date had positive Pearson correlations across all sites and sensors for ice-off (r^2 of up to 0.20, $p < 0.001$) and the largest correlations for ice-on (r^2 of up to 0.22 in the North Slope). Both mean 30-day temperature and accumulated degree day models produced weaker correlations with ice timing (r^2 falling between 0.01 and 0.12).

We also investigated the "lag timing" after the seasonal 0°C isotherm (i.e. the length of time between the 5-day 0°C isotherm and the date of ice-on/ice-off.) We found consistent negative correlation across both shoulder seasons when comparing lag duration to the date of ice-on/ice-off, indicating that lag timing is shorter in years when ice changes occur later in the season. In other words, warmer springs (those with an earlier spring 0°C isotherm) have longer lag times between the isotherm and ice-off, while warmer autumns (with a later 0°C isotherm) have shorter lag times between the isotherm and ice-on. We found that the mean ice-off lag timing fell between 16-19 days across all sites, while mean ice-on lag was shorter, between 6-13 days after the isotherm. The correlation between isotherm timing and lag days was statistically significant ($p < 0.001$) across all sites and seasons, with r^2 values ranging from 0.26 to 0.56. The slope of this relationship (i.e. the change in lag timing per change in isotherm timing) generally fell between 0.5 and 1.0 fewer lag days per day of later isotherm occurrence.



https://doi.org/10.5194/egusphere-2026-6795
Preprint. Discussion started: 19 November 2026
© Author(s) 2026. CC BY 4.0 License.

Figure 10: Relationship between the timing of the 0°C isotherm date and number of lag days for both ice-on (left column) and ice-off (right column) across our three study sites: the North Slope, Yukon Flats, and Yukon-Kuskokwim Delta. Lag time was calculated as number of days between the 0°C isotherm crossing and the corresponding ice phenology event observed in Sentinel-2 imagery. Points represent individual lake-years, while shaded density contours indicate concentration of observations. Solid regression lines indicate a strong trend (|r| > 0.7) while dashed lines denote moderate correlations (|r| > 0.4). Negative correlations indicate that later isotherm dates are associated with shorter lags to ice phenology dates. Note that corresponding Planet data was not included in this climate analysis, as we found Sentinel had higher accuracy in detecting ice phenology dates—but Planet still exhibited similar moderate correlation across all sites.

5 Discussion

5.1 Benefits and Drawbacks of High-Resolution Remote Sensing for Lake Ice Monitoring

We found that Sentinel-2 outperforms PlanetScope for lake ice monitoring at high latitudes, which we attribute to Sentinel's superior cloud masking, broader swath width, and wider spectral range. Most of the issues with Planet stemmed from the product's inability to accurately detect clouds. Planet's UDM-2 cloud mask proved to be largely unreliable; more than 51.6% of downloaded "clear" imagery was unusable in our highest latitude site due to an overarching ~15% failure rate across all seasons (Fig. 2). This finding is consistent with previous studies which found Planet's cloud mask was insufficient for time series filtering, necessitating the manual removal of cloudy scenes (John et al., 2022). We attribute this cloud detection error to the spectral limitations of PlanetScope, as both Planet's Dove (4-band) and SuperDove (8-band) lack SWIR bands which are useful in spectrally differentiating cloud from snow (Z. Li et al., 2026). Planet's high cloud mask failure rate presents a problem for commercial users of Planet data, as a large portion of image quota may be wasted on unusable scenes even when using a strict 0% cloud filter. Planet's cloud mask failure forced us to filter thousands of scenes by hand, which was a major drawback to working with the imagery in this study.

Similarly, we found that Planet's mean effective revisit rate underperformed compared to Sentinel-2 across both ice-off and ice-on in each of our higher latitude sites, the NS and YF, with significant variability in observational success year-to-year. Sentinel-2's effective revisit rates have likely exceeded Planet's performance at high latitudes since 2017 after the launch of Sentinel-2B, which cut revisit time in half, allowing for near-daily observation frequency in the high Arctic (Gascon et al., 2017; J. Li & Roy, 2017). Our findings indicate that Sentinel-2 has much more homogenous and reliable revisit timing across the Arctic, with Planet missing entire seasons in some areas, especially during ice-on (Fig. 6). In part, this difference is due to Planet's smaller swath width; a single SuperDove scene is roughly 640 km², while a single Sentinel-2 scene is 10,000 km². This nearly fifteen-times increase in spatial breadth means Sentinel more reliably and regularly captures the entirety of large study sites and can filter out scattered cloud cover to still observe a majority of lakes each pass. Additionally, we note that Planet's mass-produced CubeSats also lead to frequent georeferencing error, which can further complicate time series (Cooley

https://doi.org/10.5194/egusphere-2026-6795
Preprint. Discussion started: 19 November 2026
© Author(s) 2026. CC BY 4.0 License.

et al., 2017; Frazier & Hemingway, 2021). Georeferencing error is much less of an issue for Sentinel, which has highly stable geometric stability with sub-pixel spatial precision (Skakun et al., 2017). Despite this, Planet still exhibited meaningfully improved performance in our lowest latitude site, the YKD, as the PlanetScope flock exceeds Sentinel-2's revisit rate at lower latitudes due to orbital divergence of the smaller Sentinel-2 constellation.

Our results also suggest that Sentinel-2's spectral precision provides a meaningful advantage over PlanetScope in lake ice monitoring, particularly during ice-on. Despite Sentinel's lower spatial resolution (10 m vs Planet's ~3 m pixel size), Sentinel's random forest models outperformed or matched Planet across all tasks, even for monitoring very small lakes with a high proportion of mixed pixels. Planet's flock of CubeSats was designed to be mass produced at low cost, which means their individual spectral calibration and signal-to-noise ratio inherently lack the radiometric quality of high-budget government missions. Spectrally, Planet's original Dove and Dove-R satellites were limited to 4 bands (RGB + NIR), with 8-band SuperDove satellites beginning to take hold in November 2019. SuperDove added Coastal Blue, Yellow, Green, and Red Edge bands, but no SWIR bands, which are crucial for reliable cloud masking in snowy environments (Coluzzi et al., 2018). Alternatively, Sentinel-2 offers 13 spectral bands, spanning the visible, near-infrared, and SWIR spectrums, with specific bands included for water vapor (B9- 0.945 µm), cirrus (B10- 1.375 µm), and short-wave infrared (B11- 1.61 µm and B12- 2.19 µm) designed to aid in cloud detection. Despite its lower spatial resolution (10 m vs Planet's 3 m), Sentinel-2 has been found in numerous studies to have higher classification accuracy than Planet, including in studies focused on vegetation analysis, wildfire response, riverine pollution, smallholder farm yield, and water turbidity (Jain et al., 2022; Sunar et al., 2023; Vetrita et al., 2025; Zagajewski et al., 2024). In our study, we found that this pattern also holds for lake ice monitoring, as Sentinel-2's improved sensors were able to better detect thin ice, haze, and cloud, which more than compensated for the satellite's spatial resolution limitations.

Consequently, our findings indicate that Sentinel-2 has greater utility than Planet for high-latitude remote sensing, especially for any tasks which require accurate cloud masking. We propose that a major update to Planet's cloud mask could allow for improvement in the satellite's applicability for northern remote sensing, although we note the satellite's small swath widths, data privacy restrictions, and limited spectral bands would remain inherent drawbacks for large scale analyses at high latitudes. Despite Planet's drawbacks, we note that Planet's relative temporal advantage over Sentinel-2 greatly increased at lower latitudes, especially in low-cloud years in the YKD (Fig. 7). It is thus likely that Planet still offers major revisit rate advantages over Sentinel-2 for remote sensing at temperate and tropical latitudes, particularly in sites where clouds are easy to distinguish from underlying terrain.

5.2 Effects of Lake Morphology and Climatology on Ice Timing

Our results demonstrate that large lakes remained ice covered for 7.1 days longer on average than small lakes across all study sites, with each additional km² of lake area leading to approximately 2.4 days of additional ice duration (Fig 8). This is primarily

https://doi.org/10.5194/egusphere-2026-6795
Preprint. Discussion started: 19 November 2026
© Author(s) 2026. CC BY 4.0 License.

attributable to differences in ice-off timing associated with greater thermal inertia in the spring, since increased water volume allows for greater resistance to air temperature changes (Higgins et al., 2021). We found that ice-on was generally more synchronous than ice-off within each study site, and therefore we do not identify strong lake size patterns during the fall season. However, it is possible that greater uncertainty associated with our ice-on observations meant that small differences in ice-on timing across lake size went undetected.

Our analysis is consistent with previous research that identifies both the autumn and spring 0°C isotherms as highly correlated with lake ice phenology (Arp et al., 2013; Sharma et al., 2019; Šmejkalová et al., 2016). Although past studies have found strong latitudinal controls on ice-off timing on a regional scale (Nguyen et al., 2026), we note that on a continental scale this is not necessarily the case; the YKD and YF had nearly identical ice-off dates despite their latitudinal difference, as their annual temperature curves converge in the spring but diverge in autumn. Additionally, we found a negative correlation between the timing of the 0°C isotherm and the subsequent number of lag days before ice-off. In colder years, lakes hold onto ice for longer and therefore lose ice much more quickly after the delayed spring 0°C isotherm, when high solar angles allow for increased incoming solar radiation and therefore more rapid albedo feedback. Similar patterns have previously been analyzed by Pletcher et al. (2025) in their study of ice-off dynamics in the YKD; our results indicate that this pattern similarly holds true across the YF and NS for ice-off.

Furthermore, we present new evidence that the negative correlation between the timing of the 0°C isotherm and number of subsequent lag days is also present during ice-on. This finding has not been established from prior remote sensing studies, as ice-on dynamics remain largely understudied, especially in the optical remote sensing literature. We hypothesize that this negative correlation occurs because late isotherm dates in autumn lead to lower sun angles during delayed ice-on, and therefore more rapid cooling due to decreased insolation. This negative lag time correlation represents a non-linearity in the relationship between air temperature and ice cover which could act as a minor negative climate feedback at high latitudes. As warming leads to earlier spring 0°C isotherms and later fall 0°C isotherms, ice-off and ice-on will occur during periods with lower solar insolation and thus happen more slowly (ice-off) and more quickly (ice-on) due to reduced incoming solar energy, which may reduce the magnitude of lost ice cover days.

6 Conclusion

In this study, we present an analysis of annual ice phenology time series derived from Sentinel-2 and PlanetScope imagery for more than 15.9 million observations of 15,885 lakes across Alaska. We demonstrate that Sentinel-2 outperforms Planet for high-latitude remote sensing tasks due to its higher effective revisit rate, improved cloud masking, and superior ice classification performance. Our results indicate that each additional square km of lake area leads to approximately 2.4 days of additional annual ice duration. We also show that lake ice demonstrates a non-linearity in its response to air temperature

https://doi.org/10.5194/egusphere-2026-6795
Preprint. Discussion started: 19 November 2026
© Author(s) 2026. CC BY 4.0 License.

during both ice-on and ice-off. Overall, our study emphasizes the importance of monitoring ice dynamics in small lakes and ponds, as small water bodies are highly sensitive to climate change. Furthermore, our results highlight why public, government-backed satellite missions remain a crucial tool for climate science even with the recent growth of commercial remote sensing constellations. We propose that future studies could use Sentinel-2 to investigate the complex climactic, ecological, and morphometric variables affecting ice cover in small lakes to better understand how lakes across the world will vary in their response to climate change.

Code and data availability

Ice time series CSV files for both PlanetScope and Sentinel-2, as well as cloud and ice phenology accuracy assessments, are publicly available on Zenodo (DOI: https://doi.org/10.5281/zenodo.23897783).
The codebase for this project is also publicly available on Zenodo (DOI: https://doi.org/10.5281/zenodo.23897950).

Author contributions

N.J. and S.C. collaboratively designed the methodology for this paper. N.J. conducted the formal analysis and investigation, wrote the manuscript, and created the figures. S.C. secured the funding for this project, initially conceptualized the research, provided supervision to N.J. and A.C., and edited the manuscript. A.C. assisted with research analysis tasks like labelling and data validation.

Competing interests

The authors declare that they have no conflict of interest.

Disclaimer

Copernicus Publications remains neutral with regard to jurisdictional claims made in the text, published maps, institutional affiliations, or any other geographical representation in this paper. While Copernicus Publications makes every effort to include appropriate place names, the final responsibility lies with the authors. Views expressed in the text are those of the authors and do not necessarily reflect the views of the publisher.

https://doi.org/10.5194/egusphere-2026-6795
Preprint. Discussion started: 19 November 2026
© Author(s) 2026. CC BY 4.0 License.

Acknowledgements

This research was funded by NASA Grant #80NSSC24K1570 to S. Cooley. We acknowledge Planet Labs and the NASA CSDA program for granting access to the PlanetScope imagery used in this study. We also thank the European Space Agency for the free and open Copernicus Sentinel-2 data, and Element 84 for the Earth Search STAC Catalogue, which made this data easily accessible. The authors acknowledge that Claude was used for accelerating Python programming in this project, with sparse additions from Gemini and ChatGPT.

References

Aporta, C. (2009). The Trail as Home: Inuit and Their Pan-Arctic Network of Routes. *Human Ecology*, *37*(2), 131–146. https://doi.org/10.1007/s10745-009-9213-x

Arp, C. D., Jones, B. M., & Grosse, G. (2013). Recent lake ice-out phenology within and among lake districts of Alaska, U.S.A. *Limnology and Oceanography*, *58*(6), 2013–2028. https://doi.org/10.4319/lo.2013.58.6.2013

Arp, C. D., Jones, B. M., Liljedahl, A. K., Hinkel, K. M., & Welker, J. A. (2015). Depth, ice thickness, and ice-out timing cause divergent hydrologic responses among Arctic lakes. *Water Resources Research, 51*(12), 9379–9401. https://doi.org/10.1002/2015WR017362

Ballinger, T. J., Bhatt, U. S., Bieniek, P. A., Brettschneider, B., Lader, R. T., Littell, J. S., Thoman, R. L., Waigl, C. F., Walsh, J. E., & Webster, M. A. (2023). Alaska Terrestrial and Marine Climate Trends, 1957–2021. *Journal of Climate*, *36*(13), 4375–4391. https://doi.org/10.1175/JCLI-D-22-0434.1

Barbieux, K., Charitsi, A., & Merminod, B. (2018). Icy lakes extraction and water-ice classification using Landsat 8 OLI multispectral data. *International Journal of Remote Sensing*, *39*(11), 3646–3678. https://doi.org/10.1080/01431161.2018.1447165

Basu, A., Culpepper, J., Blagrave, K., & Sharma, S. (2024). Phenological Shifts in Lake Ice Cover Across the Northern Hemisphere: A Glimpse Into the Past, Present, and the Future of Lake Ice Phenology. *Water Resources Research*, *60*(9), e2023WR036392. https://doi.org/10.1029/2023WR036392

Biggs, J., von Fumetti, S., & Kelly-Quinn, M. (2017). The importance of small waterbodies for biodiversity and ecosystem services: Implications for policy makers. *Hydrobiologia*, *793*(1), 3–39. https://doi.org/10.1007/s10750-016-3007-0

https://doi.org/10.5194/egusphere-2026-6795
Preprint. Discussion started: 19 November 2026
© Author(s) 2026. CC BY 4.0 License.

Bonsal, B. R., & Prowse, T. D. (2003). Trends and Variability in Spring and Autumn 0 °C-Isotherm Dates over Canada. *Climatic Change*, *57*(3), 341–358. https://doi.org/10.1023/A:1022810531237

Brown, L. C., & Duguay, C. R. (2010). The response and role of ice cover in lake–climate interactions. *Progress in Physical Geography, 34*(5), 671–704. https://doi.org/10.1177/0309133310375653

Carothers, C., Brown, C., Moerlein, K. J., López, J. A., Andersen, D. B., & Retherford, B. (2014). Measuring perceptions of climate change in northern Alaska: Pairing ethnography with cultural consensus analysis. *Ecology and Society*, *19*(4). https://www.jstor.org/stable/26269670

Cold, H. S., Brinkman, T. J., Brown, C. L., Hollingsworth, T. N., Brown, D. R. N., & Heeringa, K. M. (2020). Assessing vulnerability of subsistence travel to effects of environmental change in Interior Alaska. *Ecology and Society*, *25*(1), 20. https://doi.org/10.5751/ES-11426-250120

Coluzzi, R., Imbrenda, V., Lanfredi, M., & Simoniello, T. (2018). A first assessment of the Sentinel-2 Level 1-C cloud mask product to support informed surface analyses. *Remote Sensing of Environment*, *217*, 426–443. https://doi.org/10.1016/j.rse.2018.08.009

Cooley, S. W., & Pavelsky, T. M. (2016). Spatial and temporal patterns in Arctic river ice breakup revealed by automated ice detection from MODIS imagery. *Remote Sensing of Environment*, *175*, 310–322. https://doi.org/10.1016/j.rse.2016.01.004

Cooley, S. W., Smith, L. C., Ryan, J. C., Pitcher, L. H., & Pavelsky, T. M. (2019). Arctic-Boreal Lake Dynamics Revealed Using CubeSat Imagery. *Geophysical Research Letters*, *46*(4), 2111–2120. https://doi.org/10.1029/2018GL081584

Cooley, S. W., Smith, L. C., Stepan, L., & Mascaro, J. (2017). Tracking Dynamic Northern Surface Water Changes with High-Frequency Planet CubeSat Imagery. *Remote Sensing*, *9*(12), 1306. https://doi.org/10.3390/rs9121306

Cooley, S. W., Webb, E. E., Levenson, E. S., & Ryan, J. C. (2026). Lakes Modify the Magnitude and Timing of the Northern Hemisphere Terrestrial Cryosphere Radiative Effect. *Geophysical Research Letters*, *53*(18), e2026GL124236. https://doi.org/10.1029/2026GL124236

Dolan, W., Pavelsky, T. M., & Yang, X. (2021). Functional Lake-to-Channel Connectivity Impacts Lake Ice in the Colville Delta, Alaska. *Journal of Geophysical Research: Earth Surface*, *126*(12), e2021JF006362. https://doi.org/10.1029/2021JF006362

https://doi.org/10.5194/egusphere-2026-6795
Preprint. Discussion started: 19 November 2026
© Author(s) 2026. CC BY 4.0 License.



Domart, D., Nadeau, D. F., Thiboult, A., Anctil, F., Ghobrial, T., Prairie, Y. T., Bédard-Therrien, A., & Tremblay, A. (2024). A global analysis of ice phenology for 3702 lakes and 1028 reservoirs across the Northern Hemisphere using Sentinel-2 imagery. *Cold Regions Science and Technology*, *227*, 104294. https://doi.org/10.1016/j.coldregions.2024.104294

Frazier, A. E., & Hemingway, B. L. (2021). A Technical Review of Planet Smallsat Data: Practical Considerations for Processing and Using PlanetScope Imagery. *Remote Sensing*, *13*(19), 3930. https://doi.org/10.3390/rs13193930

Gascon, F., Bouzinac, C., Thépaut, O., Jung, M., Francesconi, B., Louis, J., Lonjou, V., Lafrance, B., Massera, S., Gaudel-Vacaresse, A., Languille, F., Alhammoud, B., Viallefont, F., Pflug, B., Bieniarz, J., Clerc, S., Pessiot, L., Trémas, T., Cadau, E., … Fernandez, V. (2017). Copernicus Sentinel-2A Calibration and Products Validation Status. *Remote Sensing*, *9*(6), 584. https://doi.org/10.3390/rs9060584

Giroux-Bougard, X., Fluet-Chouinard, E., Crowley, M. A., Cardille, J. A., & Humphries, M. M. (2023). Multi-sensor detection of spring breakup phenology of Canada's lakes. *Remote Sensing of Environment*, *295*, 113656. https://doi.org/10.1016/j.rse.2023.113656

Grant, L., Vanderkelen, I., Gudmundsson, L., Tan, Z., Perroud, M., Stepanenko, V. M., Debolskiy, A. V., Droppers, B., Janssen, A. B. G., Woolway, R. I., Choulga, M., Balsamo, G., Kirillin, G., Schewe, J., Zhao, F., del Valle, I. V., Golub, M., Pierson, D., Marcé, R., … Thiery, W. (2021). Attribution of global lake systems change to anthropogenic forcing. *Nature Geoscience*, *14*(11), 849–854. https://doi.org/10.1038/s41561-021-00833-x

Gschwentner, D., & Corman, J. R. (2023). Temperature drives variability in recent satellite-derived ice cover trends in Nebraska Sand Hill lakes. *Inland Waters*, *13*(4), 545–559. https://doi.org/10.1080/20442041.2024.2327971

Guo, M., Zhuang, Q., Tan, Z., Shurpali, N., Juutinen, S., Kortelainen, P., & Martikainen, P. J. (2020). Rising methane emissions from boreal lakes due to increasing ice-free days. *Environmental Research Letters*, *15*(6), 064008. https://doi.org/10.1088/1748-9326/ab8254

Hampton, S. E., Powers, S. M., Dugan, H. A., Knoll, L. B., McMeans, B. C., Meyer, M. F., O'Reilly, C. M., Ozersky, T., Sharma, S., Barrett, D. C., Chandra, S., Jansen, J., McClure, R. P., Rautio, M., Weyhenmeyer, G. A., & Yang, X.

https://doi.org/10.5194/egusphere-2026-6795
Preprint. Discussion started: 19 November 2026
© Author(s) 2026. CC BY 4.0 License.

(2024). Environmental and societal consequences of winter ice loss from lakes. *Science*, *386*(6718), eadl3211. https://doi.org/10.1126/science.adl3211

Heinilä, K., Mattila, O.-P., Metsämäki, S., Väkevä, S., Luojus, K., Schwaizer, G., & Koponen, S. (2021). A novel method for detecting lake ice cover using optical satellite data. *International Journal of Applied Earth Observation and Geoinformation*, *104*, 102566. https://doi.org/10.1016/j.jag.2021.102566

Higgins, S. N., Desjardins, C. M., Drouin, H., Hrenchuk, L. E., & van der Sanden, J. J. (2021). The Role of Climate and Lake Size in Regulating the Ice Phenology of Boreal Lakes. *Journal of Geophysical Research: Biogeosciences*, *126*(3), e2020JG005898. https://doi.org/10.1029/2020JG005898

Holgerson, M. A., & Raymond, P. A. (2016). Large contribution to inland water CO2 and CH4 emissions from very small ponds. *Nature Geoscience*, *9*(3), 222–226. https://doi.org/10.1038/ngeo2654

Hori, Y., Gough, W. A., Butler, K., & Tsuji, L. J. S. (2017). Trends in the seasonal length and opening dates of a winter road in the western James Bay region, Ontario, Canada. *Theoretical and Applied Climatology*, *129*(3), 1309–1320. https://doi.org/10.1007/s00704-016-1855-1

Jain, M., Zhou, W., & Paliwal, A. (2022). Mapping Smallholder Yields Using Planet and Sentinel-2 Satellite Data. In K. P. Vadrevu, T. Le Toan, S. S. Ray, & C. Justice (Eds.), *Remote Sensing of Agriculture and Land Cover/Land Use Changes in South and Southeast Asian Countries* (pp. 187–199). Springer International Publishing. https://doi.org/10.1007/978-3-030-92365-5_10

Jansen, J., Thornton, B. F., Jammet, M. M., Wik, M., Cortés, A., Friborg, T., MacIntyre, S., & Crill, P. M. (2019). Climate-Sensitive Controls on Large Spring Emissions of CH4 and CO2 From Northern Lakes. *Journal of Geophysical Research: Biogeosciences*, *124*(7), 2379–2399. https://doi.org/10.1029/2019JG005094

John, A., Cannistra, A. F., Yang, K., Tan, A., Shean, D., Hille Ris Lambers, J., & Cristea, N. (2022). High-Resolution Snow-Covered Area Mapping in Forested Mountain Ecosystems Using PlanetScope Imagery. *Remote Sensing*, *14*(14), 3409. https://doi.org/10.3390/rs14143409

Jorgenson, M. T., Sedinger, J., Ely, C., Fienup-Riordan, A., Atkinson, D. E., Ayuluk, J., Brown, D., Frost, G. V., Jones, B. M., Jorgenson, J., Keim, F., Loehman, R. A., Macander, M., & Rearden, A. (2025). Interacting Sea-Level Rise,

https://doi.org/10.5194/egusphere-2026-6795
Preprint. Discussion started: 19 November 2026
© Author(s) 2026. CC BY 4.0 License.

Sea-Ice Loss, Storm Flooding, Erosion, and Permafrost Thaw Threaten Ecosystems, Wildlife, and Communities on the Yukon-Kuskokwim Delta. *Earth's Future*, *13*(8), e2025EF006015. https://doi.org/10.1029/2025EF006015

Knoll, L. B., Sharma, S., Denfeld, B. A., Flaim, G., Hori, Y., Magnuson, J. J., Straile, D., & Weyhenmeyer, G. A. (2019). Consequences of lake and river ice loss on cultural ecosystem services. *Limnology and Oceanography Letters,* 4(5), 119-131. https://doi.org/10.1002/lol2.10116

Kofinas, G. P., Chapin, F. S., III, BurnSilver, S., Schmidt, J. I., Fresco, N. L., Kielland, K., Martin, S., Springsteen, A., & Rupp, T. S. (2010). Resilience of Athabascan subsistence systems to interior Alaska's changing climate. *Canadian Journal of Forest Research, 40*(7), 1347–1359. https://doi.org/10.1139/X10-108

Korver, M. C., Lehner, B., Cardille, J. A., & Carrea, L. (2024). Surface water temperature observations and ice phenology estimations for 1.4 million lakes globally. *Remote Sensing of Environment*, *308*, 114164. https://doi.org/10.1016/j.rse.2024.114164

Kouraev, A. V., Zakharova, E. A., Kostianoy, A. G., Shimaraev, M. N., Desinov, L. V., Petrov, E. A., Hall, N. M. J., Rémy, F., & Suknev, A. Y. (2021). Giant ice rings in southern Baikal: Multi-satellite data help to study ice cover dynamics and eddies under ice. *The Cryosphere*, *15*(9), 4501–4516. https://doi.org/10.5194/tc-15-4501-2021

Kuhn, C., John, A., Hille Ris Lambers, J., Butman, D., & Tan, A. (2021). Arctic-Boreal Lake Phenology Shows a Relationship between Earlier Lake Ice-Out and Later Green-Up. *Remote Sensing*, *13*(13), 2533. https://doi.org/10.3390/rs13132533

Kuhn, M., Olefeldt, D., Arndt, K. A., Bastviken, D., Bruhwiler, L., Crill, P., DelSontro, T., Fluet-Chouinard, E., Grosse, G., Hovemyr, M., Hugelius, G., MacIntyre, S., Malhotra, A., McGuire, A. D., Oh, Y., Poulter, B., Treat, C. C., Turetsky, M. R., Varner, R. K., … Zhang, Z. (2025). Current and future methane emissions from boreal-Arctic wetlands and lakes. *Nature Climate Change*, *15*(9), 986–991. https://doi.org/10.1038/s41558-025-02413-y

Levenson, E. S., Cooley, S. W., Mullen, A. L., Webb, E. E., & Watts, J. D. (2025). Glacial History Modifies Permafrost Controls on the Distribution of Lakes and Ponds. *Geophysical Research Letters*, *52*(4), e2024GL112771. https://doi.org/10.1029/2024GL112771

Levenson, E. S., Cooley, S. W., & Mullen, A. L. (2024). ABoVE: Alaska Lake and Pond Occurrence (Version 1). ORNL Distributed Active Archive Center. https://doi.org/10.3334/ORNLDAAC/2399

https://doi.org/10.5194/egusphere-2026-6795
Preprint. Discussion started: 19 November 2026
© Author(s) 2026. CC BY 4.0 License.

Li, J., & Roy, D. P. (2017). A Global Analysis of Sentinel-2A, Sentinel-2B and Landsat-8 Data Revisit Intervals and Implications for Terrestrial Monitoring. *Remote Sensing*, *9*(9), 902. https://doi.org/10.3390/rs9090902

Li, X., Peng, S., Xi, Y., Woolway, R. I., & Liu, G. (2022). Earlier ice loss accelerates lake warming in the Northern Hemisphere. *Nature Communications*, *13*(1), 5156. https://doi.org/10.1038/s41467-022-32830-y

Li, Z., Xie, Y., Skakun, S., Jia, X., Mai, G., Lu, W., Tong, M., & Wang, Z. (2026). Annotation-free cloud masking for PlanetScope images in the Arctic via cross-platform ability transfer using deep learning and foundation models. *Remote Sensing of Environment*, *334*, 115138. https://doi.org/10.1016/j.rse.2025.115138

Liu, C., Huang, H., Hui, F., Zhang, Z., & Cheng, X. (2021). Fine-Resolution Mapping of Pan-Arctic Lake Ice-Off Phenology Based on Dense Sentinel-2 Time Series Data. *Remote Sensing*, *13*(14), 2742. https://doi.org/10.3390/rs13142742

Martinsen, K. T., Kragh, T., & Sand-Jensen, K. (2019). Carbon dioxide efflux and ecosystem metabolism of small forest lakes. *Aquatic Sciences*, *82*(1), 9. https://doi.org/10.1007/s00027-019-0682-8

Mizukami, N., Newman, A. J., Littell, J. S., Giambelluca, T. W., Wood, A. W., Gutmann, E. D., Hamman, J. J., Gergel, D. R., Nijssen, B., Clark, M. P., & Arnold, J. R. (2022). New projections of 21st century climate and hydrology for Alaska and Hawai‘i. *Climate Services*, *27*, 100312. https://doi.org/10.1016/j.cliser.2022.100312

Moerlein, K. J., & Carothers, C. (2012). Total Environment of Change: Impacts of Climate Change and Social Transitions on Subsistence Fisheries in Northwest Alaska. *Ecology and Society*, *17*(1). https://www.jstor.org/stable/26268996

Mullan, D. J., Barr, I. D., Flood, R. P., Galloway, J. M., Newton, A. M. W., & Swindles, G. T. (2021). Examining the viability of the world's busiest winter road to climate change using a process-based lake model. *Bulletin of the American Meteorological Society, 102*(7), E1464–E1480. https://doi.org/10.1175/BAMS-D-20-0168.1

Mullen, A. L, Watts, J. D., Rogers, B. M., Carroll, M. L., Elder, C. D., Noomah, J., Williams, Z., Caraballo-Vega, J. A., Bredder, A., Rickenbaugh, E., Levenson, E. S., Cooley, S. W., Hung, J. K. Y., Fiske, G., Potter, S., Yang, Y., Miller, C. E., Natali, S. M., Douglas, T. A., & Kyzivat, E. D. (2023). Using High-Resolution Satellite Imagery and Deep Learning to Track Dynamic Seasonality in Small Water Bodies. *Geophysical Research Letters*, *50*(7), e2022GL102327. https://doi.org/10.1029/2022GL102327

https://doi.org/10.5194/egusphere-2026-6795
Preprint. Discussion started: 19 November 2026
© Author(s) 2026. CC BY 4.0 License.

Nguyen, A. L., Lopez, C. G., Melara-Valle, J., Ross, E., Bradley, A. S., Limbeck, M. R., Masteller, C. C., & Michaelides, R. (2026). *Multi-sensor satellite analysis reveals latitudinal and morphometric controls on ice phenology across 31,000 thermokarst lakes on the Alaska North Slope* [Preprint]. EGUsphere. https://doi.org/10.5194/egusphere-2026-1135

Nitze, I., Grosse, G., Jones, B. M., Arp, C. D., Ulrich, M., Fedorov, A., & Veremeeva, A. (2017). Landsat-based trend analysis of lake dynamics across northern permafrost regions. *Remote Sensing, 9*(7), 640. https://doi.org/10.3390/rs9070640

Pavelsky, T. M., & Smith, L. C. (2004). Spatial and temporal patterns in Arctic river ice breakup observed with MODIS and AVHRR time series. *Remote Sensing of Environment*, *93*(3), 328–338. https://doi.org/10.1016/j.rse.2004.07.018

Pi, X., Luo, Q., Feng, L., Xu, Y., Tang, J., Liang, X., Ma, E., Cheng, R., Fensholt, R., Brandt, M., Cai, X., Gibson, L., Liu, J., Zheng, C., Li, W., & Bryan, B. A. (2022). Mapping global lake dynamics reveals the emerging roles of small lakes. *Nature Communications*, *13*(1), 5777. https://doi.org/10.1038/s41467-022-33239-3

Pickens, A. H., Hansen, M. C., Stehman, S. V., Tyukavina, A., Potapov, P., Zalles, V., & Higgins, J. (2022). Global seasonal dynamics of inland open water and ice. *Remote Sensing of Environment*, *272*, 112963. https://doi.org/10.1016/j.rse.2022.112963

Pletcher, A., Cooley, S. W., & Levenson, E. S, (2025). Observing Fine-Scale Lake Ice-Out Dynamics in the Lower Kuskokwim River Basin, Alaska. *Hydrological Processes*, *39*(11), e70309. https://doi.org/10.1002/hyp.70309

Rey, D. M., Walvoord, M., Minsley, B., Rover, J., & Singha, K. (2019). Investigating lake-area dynamics across a permafrost-thaw spectrum using airborne electromagnetic surveys and remote sensing time-series data in Yukon Flats, Alaska. *Environmental Research Letters*, *14*(2), 025001. https://doi.org/10.1088/1748-9326/aaf06f

Schott, S., Qitsualik, J., Van Coeverden de Groot, P., Okpakok, S., Chapman, J. M., Lougheed, S., & Walker, V. K. (2020). Operationalizing knowledge coevolution: Towards a sustainable fishery for Nunavummiut. *Arctic Science*, *6*(3), 208–228. https://doi.org/10.1139/as-2019-0011

Seekell, D., Cael, B. B., & Byström, P. (2022). Problems With the Shoreline Development Index—A Widely Used Metric of Lake Shape. *Geophysical Research Letters*, *49*(10), e2022GL098499. https://doi.org/10.1029/2022GL098499

https://doi.org/10.5194/egusphere-2026-6795
Preprint. Discussion started: 19 November 2026
© Author(s) 2026. CC BY 4.0 License.

Seigle, J. C., Prichard, A. K., Gall, A. E., & Nukapigak, T. (2024). Factors influencing harvest success for an Arctic under-ice subsistence fishery. *Polar Science*, *42*, 101126. https://doi.org/10.1016/j.polar.2024.101126

Sharma, S., Blagrave, K., Magnuson, J. J., O'Reilly, C. M., Oliver, S., Batt, R. D., Magee, M. R., Straile, D., Weyhenmeyer, G. A., Winslow, L., & Woolway, R. I. (2019). Widespread loss of lake ice around the Northern Hemisphere in a warming world. *Nature Climate Change*, *9*(3), 227–231. https://doi.org/10.1038/s41558-018-0393-5

Skakun, S., Vermote, E., Roger, J.-C., & Justice, C. (2017). Multispectral Misregistration of Sentinel-2A Images: Analysis and Implications for Potential Applications. *IEEE Geoscience and Remote Sensing Letters*, *14*(12), 2408–2412. https://doi.org/10.1109/LGRS.2017.2766448

Šmejkalová, T., Edwards, M. E., & Dash, J. (2016). Arctic lakes show strong decadal trend in earlier spring ice-out. *Scientific Reports*, *6*(1), 38449. https://doi.org/10.1038/srep38449

Smol, J. P., & Douglas, M. S. V. (2007). Crossing the final ecological threshold in high Arctic ponds. *Proceedings of the National Academy of Sciences*, *104*(30), 12395–12397. https://doi.org/10.1073/pnas.0702777104

Sunar, F., Dervisoglu, A., Yagmur, N., Aslan, E., & Ozguven, M. (2023). Analyzing the retrieval accuracy of optically active water components from satellite data under varying image resolutions. *The International Archives of the Photogrammetry, Remote Sensing and Spatial Information Sciences*, *XLVIII-M-1–2023*, 595–600. https://doi.org/10.5194/isprs-archives-XLVIII-M-1-2023-595-2023

Surdu, C. M., Duguay, C. R., Pour, H. K., & Brown, L. C. (2015). Ice Freeze-up and Break-up Detection of Shallow Lakes in Northern Alaska with Spaceborne SAR. *Remote Sensing*, *7*(5), 6133–6159. https://doi.org/10.3390/rs70506133

Tong, J., Lin, Y., Fan, C., Liu, K., Chen, T., Zeng, F., Zhan, P., Ke, L., Gao, Y., & Song, C. (2024). Fine-scale monitoring of lake ice phenology by synthesizing remote sensed and climatologic features based on high-resolution satellite constellation and modeling. *Science of The Total Environment*, *912*, 169002. https://doi.org/10.1016/j.scitotenv.2023.169002

Vetrita, Y., Diwyacitta, K., Sukarno, K. M., Albar, I., Usman, A. B., Ritonga, R. P., Santoso, I., Lestari, A. I., Kartika, T., Novresiandi, D. A., Prasasti, I., Ulfa, K., Novita, N., Siwi, S. E., Augusto, S., Prakoso, E. T., Rahmi, K. I. N., Nugroho, U. C., Widodo, J., & Cochrane, M. A. (2025). Evaluating the capabilities of high-resolution PlanetScope

https://doi.org/10.5194/egusphere-2026-6795
Preprint. Discussion started: 19 November 2026
© Author(s) 2026. CC BY 4.0 License.

and Sentinel-2 images for mapping burned area and vegetation regrowth in Indonesia's savannas. *International Journal of Remote Sensing*, *46*(18), 6803–6825. https://doi.org/10.1080/01431161.2025.2546154

Wang, X., Feng, L., Gibson, L., Qi, W., Liu, J., Zheng, Y., Tang, J., Zeng, Z., & Zheng, C. (2021). High-Resolution Mapping of Ice Cover Changes in Over 33,000 Lakes Across the North Temperate Zone. *Geophysical Research Letters*, *48*(18), e2021GL095614. https://doi.org/10.1029/2021GL095614

Wang, X., Feng, L., Qi, W., Cai, X., Zheng, Y., Gibson, L., Tang, J., Song, X., Liu, J., Zheng, C., & Bryan, B. A. (2022). Continuous Loss of Global Lake Ice Across Two Centuries Revealed by Satellite Observations and Numerical Modeling. *Geophysical Research Letters*, *49*(12), e2022GL099022. https://doi.org/10.1029/2022GL099022

Wendler, G., Gordon, T., & Stuefer, M. (2017). On the Precipitation and Precipitation Change in Alaska. *Atmosphere*, *8*(12), 253. https://doi.org/10.3390/atmos8120253

Wik, M., Varner, R. K., Anthony, K. W., MacIntyre, S., & Bastviken, D. (2016). Climate-sensitive northern lakes and ponds are critical components of methane release. *Nature Geoscience*, *9*(2), 99–105. https://doi.org/10.1038/ngeo2578

Woolway, R. I., Huang, L., Sharma, S., Lee, S.-S., Rodgers, K. B., & Timmermann, A. (2022). Lake Ice Will Be Less Safe for Recreation and Transportation Under Future Warming. *Earth's Future*, *10*(10), e2022EF002907. https://doi.org/10.1029/2022EF002907

Wright, N., Duncan, J. M. A., Callow, J. N., Thompson, S. E., & George, R. J. (2025). Training sensor-agnostic deep learning models for remote sensing: Achieving state-of-the-art cloud and cloud shadow identification with OmniCloudMask. *Remote Sensing of Environment*, *322*, 114694. https://doi.org/10.1016/j.rse.2025.114694

Wu, Y., Duguay, C. R., & Xu, L. (2021). Assessment of machine learning classifiers for global lake ice cover mapping from MODIS TOA reflectance data. *Remote Sensing of Environment*, *253*, 112206. https://doi.org/10.1016/j.rse.2020.112206

Yang, X., Pavelsky, T. M., Bendezu, L. P., & Zhang, S. (2022). Simple Method to Extract Lake Ice Condition From Landsat Images. *IEEE Transactions on Geoscience and Remote Sensing*, *60*, 1–10. https://doi.org/10.1109/TGRS.2021.3088144

https://doi.org/10.5194/egusphere-2026-6795
Preprint. Discussion started: 19 November 2026
© Author(s) 2026. CC BY 4.0 License.



Zagajewski, B., Kluczek, M., Zdunek, K. B., & Holland, D. (2024). Sentinel-2 versus PlanetScope Images for Goldenrod Invasive Plant Species Mapping. *Remote Sensing*, *16*(4), 636. https://doi.org/10.3390/rs16040636

Zhang, S., & Pavelsky, T. M. (2019). Remote Sensing of Lake Ice Phenology across a Range of Lakes Sizes, ME, USA. *Remote Sensing*, *11*(14), 1718. https://doi.org/10.3390/rs11141718

Zhang, S., Pavelsky, T. M., Arp, C. D., & Yang, X. (2021). Remote sensing of lake ice phenology in Alaska. *Environmental Research Letters*, *16*(6), 064007. https://doi.org/10.1088/1748-9326/abf965

Zhuang, X., Liu, X., Xu, S., Wang, X., Shah, A. A., Wang, L., Wu, S., Jiang, C., Ouyang, Z., & Piao, S. (2026). Human amplification of climate-induced greenhouse gas emissions from global small water bodies. *Proceedings of the National Academy of Sciences*, *123*(22), e2537678123. https://doi.org/10.1073/pnas.2537678123